Title

The evolution of white matter microstructural changes after mild traumatic brain injury: A longitudinal DTI and NODDI study.

Journal

Science advances, 6(32)

ISSN

2375-2548

Authors

Palacios, EM
Owen, JP
Yuh, EL
et al.

Publication Date

2020-08-01

DOI

10.1126/sciadv.aaz6892

NEUROSCIENCE

The evolution of white matter microstructural changes after mild traumatic brain injury: A longitudinal DTI and NODDI study

E. M. Palacios[1], J. P. Owen[2], E. L. Yuh[1,3], M. B. Wang[1], M. J. Vassar[3,4], A. R. Ferguson[3,4,5], R. Diaz-Arrastia[6], J. T. Giacino[7,8], D. O. Okonkwo[9], C. S. Robertson[10], M. B. Stein[11,12], N. Temkin[13], S. Jain[12], M. McCrea[14], C. L. MacDonald[13], H. S. Levin[15], G. T. Manley[3,4], P. Mukherjee[1,3,16]*, TRACK-TBI Investigators†

Neuroimaging biomarkers that can detect white matter (WM) pathology after mild traumatic brain injury (mTBI) and predict long-term outcome are needed to improve care and develop therapies. We used diffusion tensor imaging (DTI) and neurite orientation dispersion and density imaging (NODDI) to investigate WM microstructure cross-sectionally and longitudinally after mTBI and correlate these with neuropsychological performance. Cross-sectionally, early decreases of fractional anisotropy and increases of mean diffusivity corresponded to WM regions with elevated free water fraction on NODDI. This elevated free water was more extensive in the patient subgroup reporting more early postconcussive symptoms. The longer-term longitudinal WM changes consisted of declining neurite density on NODDI, suggesting axonal degeneration from diffuse axonal injury for which NODDI is more sensitive than DTI. Therefore, NODDI is a more sensitive and specific biomarker than DTI for WM microstructural changes due to mTBI that merits further study for mTBI diagnosis, prognosis, and treatment monitoring.

INTRODUCTION

Despite increasing evidence from preclinical and human studies that mild traumatic brain injury (mTBI) causes axonal shearing injury of white matter (WM) microstructure that can affect the long-term cognitive, neuropsychiatric, and social domains of function, the lack of reliable objective tools to measure this pathology is a barrier to clinical translation (*1*–*4*). The common assumption, even among health care professionals, that patients with mTBI will return to premorbid levels of function shortly after the traumatic event often results in these patients not receiving appropriate follow-up care after the acute injury.

Diffusion tensor imaging (DTI) is the most extensively used technique worldwide to study the microstructural properties of WM of the central nervous system (CNS) in vivo (*5*–*7*). DTI studies of mTBI have shown microstructural WM disruption that can lead to neurocognitive and behavioral deficits after mTBI (*8*–*10*). However, traditional DTI metrics such as mean diffusivity (MD) and fractional anisotropy (FA) represent basic statistical descriptions of diffusion that do not directly correspond to biophysically meaningful parameters of the underlying tissue. Furthermore, DTI assumes Gaussian diffusion within a single microstructural compartment and is therefore insensitive to the complexity of WM microstructure, which requires a non-Gaussian model with multiple compartments (*11*). Perhaps as a result, prior DTI studies have produced conflicting results, with some papers reporting abnormally reduced WM FA in mTBI and others reporting elevations or no change in FA (*12*). Other contributing factors to this discordance in the literature include small effect sizes of DTI changes due to mTBI, cross-sectional studies with small sample sizes (<40 patients), and the dynamic nature of microstructural WM alterations after mTBI.

In this investigation, we overcome the limitations of DTI by applying a more advanced multicompartment diffusion model known as neurite orientation dispersion and density imaging (NODDI) (*13*, *14*). NODDI leverages recent progress in high-performance magnetic field gradients for magnetic resonance imaging (MRI) scanners that can achieve diffusion-weighting factors much higher than the standard $b = 1000$ s/mm^2 for DTI and therefore probe more complex non-Gaussian properties of WM diffusion. The NODDI biophysical model uses this richer diffusion imaging data to measure properties of three microstructural environments: intracellular, extracellular, and free water. One such metric is the intracellular volume fraction, referred to as the neurite density index (NDI), which primarily represents axonal density within WM. Another is orientation dispersion index (ODI) of neurites, which is higher in loosely organized WM and lower in tracts with largely parallel fiber bundles such as the corpus callosum (CC). The volume fraction of the isotropic diffusion compartment (FISO) represents the free water content within the tissue (*13*). "Free water" refers to the unhindered and unrestricted diffusion of water molecules such as would be found in cerebrospinal fluid and in extracellular tissue edema. These NODDI parameters have been validated in histopathological studies of animal

[1]Department of Radiology & Biomedical Imaging, UCSF, San Francisco, CA, USA. [2]Department of Radiology, University of Washington, Seattle, WA, USA. [3]Brain and Spinal Cord Injury Center, Zuckerberg San Francisco General Hospital and Trauma Center, San Francisco, CA, USA. [4]Department of Neurological Surgery, UCSF, San Francisco, CA, USA. [5]San Francisco Veterans Affairs Medical Center, San Francisco, CA, USA. [6]Department of Neurology, University of Pennsylvania, Philadelphia, PA, USA. [7]Department of Physical Medicine and Rehabilitation, Spaulding Rehabilitation Hospital, Charlestown, MA, USA. [8]Department of Physical Medicine and Rehabilitation, Harvard Medical School, Boston, MA, USA. [9]Department of Neurological Surgery, University of Pittsburgh Medical Center, Pittsburgh, PA, USA. [10]Department of Neurosurgery, Baylor College of Medicine, Houston, TX, USA. [11]Department of Psychiatry, University of California, San Diego, La Jolla, CA, USA. [12]Department of Family Medicine & Public Health, University of California, San Diego, La Jolla, CA, USA. [13]Department of Neurological Surgery, University of Washington, Seattle, WA, USA. [14]Departments of Neurosurgery and Neurology, Medical College of Wisconsin, Milwaukee, WI, USA. [15]Department of Neurology, Baylor College of Medicine, Houston, TX, USA. [16]Department of Bioengineering and Therapeutic Sciences, University of California, San Francisco, San Francisco, CA, USA.
*Corresponding author. Email: pratik.mukherjee@ucsf.edu
†See the Supplementary Materials.

and human brains (*15*, *16*) and have been used to study brain development (*17*, *18*) and to detect subtle brain damage in other disorders (*19*–*23*).

To translate newly discovered scientific results to clinical settings, replication and generalization are essential (*24*). Therefore, neuroimaging findings must be reproducible in an independent dataset, preferably one acquired under different real-world conditions—such as scanner manufacturer, diffusion acquisition sequence, and diffusion MRI acquisition parameters—to demonstrate robustness to this variation that occurs across imaging centers. Moreover, in contrast to previous mostly cross-sectional studies, we present here a longitudinal study of two independent cohorts of 40 patients each to address the aforementioned reproducibility.

In this study, we aimed to (i) investigate the evolution of WM changes after mTBI over time by using DTI and NODDI, (ii) explore the prognostic significance of these WM microstructural changes for symptomatic and cognitive outcome after mTBI, and (iii) replicate the longitudinal arm of the study with a separate validation dataset acquired under different conditions to demonstrate reproducibility and generalizability of the results. Comparing DTI to NODDI serially after mTBI, we hypothesize that the early microstructural WM changes of mTBI would be driven by increases in free water due to vasogenic edema, whereas longer-term degenerative changes would be reflected by decreases in axonal density.

MATERIALS AND METHODS

All participants were enrolled at Zuckerberg San Francisco General Hospital and Trauma Center as part of the prospective Transforming Research and Clinical Knowledge in Traumatic Brain Injury project (TRACK-TBI) (*25*). A total sample of 40 patients with mTBI (age: $\bar{x}$ = 30.35 years, SD ± 7.50; education: $\bar{x}$ = 15 years, SD ± 2.68; sex: 9 females/31 males) was included within 24 hours after injury upon meeting the American Congress of Rehabilitation Medicine (*26*) criteria for mTBI in which the patient has to exhibit a traumatically induced physiological disruption of brain function as manifested by (i) any period of loss of consciousness (LOC), (ii) any loss of memory for events immediately before or after the accident, (iii) any alteration of mental state at the time of the accident (feeling dazed, disoriented, and/or confused), or (iv) focal neurologic deficits that may or may not be permanent. Other inclusion criteria were age between 18 and 55 years, brain computed tomography (CT) as part of clinical care within 24 hours of injury, no substantial polytrauma that would interfere with the follow-up and outcome assessment, and no MRI contraindication. Fifteen patients reported history of anxiety or depression, but none had a history of major psychiatric or neurological disorders. Visual acuity and hearing adequate for outcomes testing, fluency in English, and ability to give informed consent were required. Galveston Orientation and Amnesia Test score assessed at the time of informed consent was normal ($\bar{x}$ = 98.63, SD ± 2.18). A second longitudinal matched cohort of 40 patients with mTBI (age: $\bar{x}$ = 34.38 years, SD ± 11; education: $\bar{x}$ = 15.6 years, SD ± 2.1; sex: 11 females /28 males) was included for replication and generalization purposes from the same TRACK-TBI project and recruitment criteria. Of the initial cohort of patients with mTBI, 9 of 40 reported having a previous mTBI. From the replication cohort, 12 of 40 patients reported a previous mTBI.

Fourteen orthopedic trauma control subjects ("trauma controls") matched by age ($\bar{x}$ = 31.71 years, SD ± 10.14), education ($\bar{x}$ = 15.5 years, SD ± 2.17), and sex (six females/ eight males) were also recruited from the emergency department. Orthopedic injury causes included falls, pedestrian run overs, and bike accidents. All subjects presented with lower extremity fractures except for one with an upper extremity fracture. Orthopedic controls were ruled out for the current study if the emergency room physician required CT scan for suspicion of head trauma; if, by interviewing medical services or subjects, participants reported clinical information such as LOC, amnesia, previous TBI, psychiatric, or neurological prevalent pathology; and if, according to the abbreviated injury scale, this study would be counterproductive for their sustained systemic injuries. In addition, however, we also recruited a group of 19 healthy controls without systemic injuries ($\bar{x}$ = 36.33 years, SD ± 13.5), matched for education ($\bar{x}$ = 16.11 years, SD ± 2.13), and sex (6 females/13 males) to be compared to the initial mTBI cohort. This group was recruited from friends and family relatives of the patients and will be referred as "friend controls."

These two control groups, trauma controls and friend controls, serve to ensure that any differences with the patient cohort are reproducible and generalizable across participants without recent trauma history and also those with recent trauma not related to the brain. All eligible subjects who voluntarily agreed to participate gave written informed consent. All study protocols were approved by the University of California, San Francisco Institutional Review Board.

Neuropsychological assessment

Commonly affected neuropsychological domains after mTBI were assessed using self-report and performance-based cognitive measures at 2 weeks and 6 month after injury: (i) The Rivermead Postconcussion Symptoms Questionnaire (RPQ), a self-reported questionnaire consisting of 16 physical and psychosocial symptoms frequently reported after mTBI; (ii) the Rey Auditory Verbal Learning Test (RAVLT) to evaluate learning short- and long-term memory; (iii) Trail Making Tests A (TMTA) and B (TMTB) to evaluate attention, processing speed, and cognitive flexibility to switch tasks (TMTB-A); and (iv) the Wechsler Adult Intelligence Scale (WAIS) coding and symbol search subscales for processing speed and visuo-perceptive association learning (*27*). All measures were the raw scores.

Image acquisition

All mTBI subjects of the initial cohort were scanned on a 3T GE MR750 equipped with an 8-channel phased array head radiofrequency coil (GE Healthcare, Waukesha, WI) at 2 weeks ($\bar{x}$ = 13.30 days, SD ± 2.10) and 6 months ($\bar{x}$ = 184 days, SD ± 8.86) after injury. Whole-brain diffusion MRI was performed with a multislice single-shot spin-echo echoplanar pulse sequence (echo time [TE] = 81 ms and repetition time [TR] = 9 s) using 64 diffusion-encoding directions, isotropically distributed over the surface of a sphere with electrostatic repulsion, acquired at b = 1300 s/mm^2, another 64 directions at b = 3000 s/mm^2, and eight acquisitions at b = 0 s/mm^2 for each set of 64 diffusion-weighted directions, each slice with a thickness of 2.7 mm with no gap between slices, a 128 × 128 matrix, and a field of view (FOV) of 350 mm by 350 mm, resulting in 2.7-mm isotropic voxels. Sagittal three-dimensional (3D) inversion recovery fast spoiled gradient recalled echo T1-weighted images (inversion time [TI] = 400 ms and flip angle = 11°) were acquired with 256-mm FOV and 200 contiguous partitions (1.2 mm) at 256 × 256 matrix. Sagittal 3D gradient echo T2*-weighted images (TE = 250 ms, TR = 500 ms, and flip angle = 10°) were acquired with 256-mm FOV and

130 contiguous slices (1.6 mm) at 192 × 192 matrix. Sagittal 3D T2-weighted fluid-attenuated inversion recovery images (FLAIR; TE = 102 ms, TR = 5750 ms, and TI = 1630 ms) were acquired with 256-mm FOV and 184 contiguous slices (1.2 mm) at 256 × 256 matrix. The control group scans were acquired with the same parameters of acquisition as the mTBI patients, with data available for this study at the 2-week time point after orthopedic injury for the trauma control group.

The replication patient dataset, consisting of the second longitudinal mTBI cohort, was acquired on a 3T Siemens Magnetom Skyra scanner equipped with a 32-channel phased array head radiofrequency coil. Whole-brain diffusion MRI was performed with single-shot spin-echo EPI (echo-planar imaging) images at a multiband factor of 3 (TE = 94 ms and TR = 2.9 s) using 64 diffusion-encoding directions acquired at b = 1000 s/mm^2 and another 64 directions at b = 3000 s/mm^2, each slice with a thickness of 2.4 mm with no gap between slices, a 96 × 96 matrix, and a FOV of 230 × 230 mm. The diffusion MRI sequence also included both forward and reverse phase encoding for eight b = 0 s/mm^2 image volumes for each of the two diffusion-weighted shells. Differences in scanner manufacturer, diffusion acquisition sequence, and diffusion acquisition parameters from the first mTBI patient cohort serve to ensure that any results are robust to variation in these factors that can differ across institutions.

MRI image processing and analysis

See Fig. 1 for overview of imaging methods. This study included (i) cross-sectional group comparison analysis of the initial cohort of patients with mTBI versus the group of orthopedic trauma controls (N = 14), (ii) cross-sectional group comparison analysis of the initial cohort of patients with mTBI versus the group of friend controls (N = 19), (iii) longitudinal comparison analysis at 2 weeks versus 6 months after injury of initial cohort patients with mTBI (N = 40), (iv) longitudinal comparison at 2 weeks versus 6 months after injury of replication cohort patients with mTBI (N = 40), and (v) machine learning analysis of cognitive/behavioral recovery in both longitudinal mTBI cohorts and in relation with the imaging at 2 weeks versus 6 months after injury.

Radiological findings

Structural MRI images were interpreted by a board-certified neuroradiologist (E.L.Y) who was blinded to the initial presentation and subject group designation using the National Institutes of Health (NIH) Common Data Elements (CDEs) for TBI pathoanatomic classification (*28*). Table S1 summarizes the neuroradiological findings on structural 3T MRI for both cohorts of patients with mTBI. The MRI scans for the control group had no findings specific for TBI.

Diffusion tensor imaging

The diffusion MRI data were verified to be free of major image artifacts or excessive patient movement, defined as more than 2 mm of translation and/or rotation. DTI preprocessing and analysis were performed using tools from the Oxford Centre for Functional MRI of the Brain (FMRIB) software library, abbreviated as FSL (version 5.0.7). First, images were corrected for eddy distortions and motion using an average of the eight b = 0 s/mm^2 volumes for each diffusion-weighted shell as a reference. The registered images were skull-stripped using the Brain Extraction Tool (*29*). All the resulting brain masks were visually inspected for anatomic fidelity. DTI parameters maps were calculated using the FSL Diffusion Toolbox.

Multicompartment biophysical modeling of diffusion MR imaging

NODDI metrics were derived using the NODDI toolbox v0.9 (www.nitrc.org/projects/noddi_toolbox). We averaged the corresponding eight b = 0 s/mm^2 images for each diffusion weighting. The NODDI code was modified to account for the slightly differing minimum TE between images acquired at b = 1300 s/mm^2 versus b = 3000 s/mm^2 by fitting the NODDI model to the normalized diffusion-weighted images instead of the raw images (*30*). As per the developers' recommendation, the diffusion-weighted images at each b value were normalized by the mean b = 0 s/mm^2 images acquired with the same minimal TE scan parameter, generating images with TE-independent signal intensity, as we have described previously (*17*, *30*). NODDI fitting was performed with the NODDI MATLAB Toolbox using the default settings (www.nitrc.org/projects/noddi_toolbox, v0.9). Maps of NDI, ODI, and FISO were generated.

Statistics

Tract-based spatial statistics WM voxelwise analysis

After calculation of the FA map, a voxelwise statistical analysis of the FA data was performed using tract-based spatial statistics (TBSS). FA data were aligned into the common FMRIB58 FA template, which is in MNI152 (Montreal Neurological Institute) standard space, using the nonlinear registration algorithm FNIRT (*31*). Next, a mean FA image was created from the images for all the subject's serial scans in this common space and thinned to generate a mean FA WM skeleton that represented the center of all tracts common to the entire group of scans and thresholded at > 0.2. The aligned FA volume was then projected onto the skeleton by filling the skeleton with FA values from the nearest relevant tract center. Output images and the 0.2 thresholded skeleton were visually inspected for accuracy.

TBSS WM regions-of-interest–based analysis

Twelve main fasciculi were studied using masks obtained from the Johns Hopkins University (JHU) white-matter tractography atlas, mapped onto the standard MNI152 space, and resampled to 1-mm resolution. Binary mask images from the fasciculi of interest were used to mask the individual skeletonized maps previously registered to the MNI standard space using the nonlinear tools in the TBSS procedure. Mean FA, MD, ODI, NDI, and FISO values were obtained from each subject's WM skeleton and each of the skeletonized regions of interest. Right and left tracts were averaged into one single measurement.

We compared between subjects using a voxelwise general linear model (GLM) analysis with permutation testing to correct for multiple comparisons (*32*) using threshold-free cluster enhancement (TFCE), familywise error (FWE) corrected at $P \leq 0.05$. An unpaired t test was used to cross-sectionally compare the group of patients and controls in the voxelwise analysis at 2 weeks. A paired t test was used to compare differences among DTI and NODDI measures within the patient group between 2 weeks and 6 months.

Machine learning analysis

Many patients with mTBI remain functionally impaired long-term after injury (*33*). In an attempt to distinguish these patients in our cohort, we used unsupervised machine learning to derive a metric of cognitive and symptom improvement and link it to the imaging

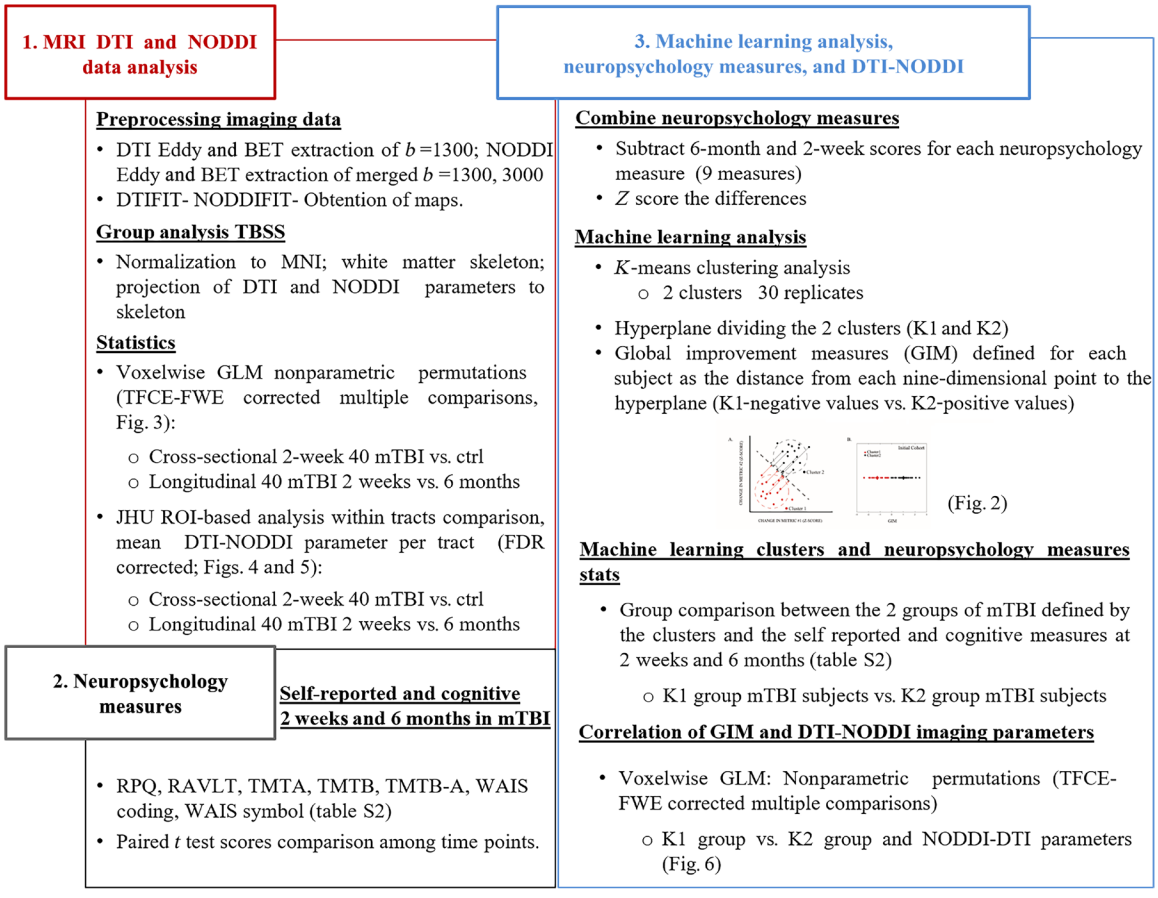

Fig. 1. Overview of the imaging analysis and statistical methods.

biomarkers. First, to obtain and define a global improvement measure (GIM) that best reflects their outcomes, we first subtracted the 2-week scores from the 6-month scores for each of the nine self-reported and cognitive measures described in table S2 for each subject and then used a *Z* score transformation to normalize the values. Because each individual test could be noisy, we sought to combine them together into a single composite metric that we defined as the GIM. We approached this task through an unsupervised *k*-means clustering analysis with 2 clusters and 30 replicates in MATLAB 2012b (The MathWorks Inc., Natick, MA, USA). We then calculated a hyperplane to separate these two clusters equidistantly, and each subject's GIM was defined as the signed (positive/negative) distance between the subject's recovery status and this hyperplane. This distance can also be expressed as a weighted average of the various symptomatic and cognitive metrics (Fig. 2A). Intuitively, this represents a data-driven method to combine the various self-reported and cognitive performance-based metrics to provide a wide degree of discrimination between patient outcome groups. We used two clusters because we were interested in distinguishing the patients with the best improvement from those who did not improve. While one cluster represents patients whose testing trend indicates overall improvement between 2 weeks and 6 months, the other cluster represents patients whose overall testing indicates a lack of improvement or, in some cases, a regression of testing performance. Last, we performed the voxelwise comparison among clusters determined by the GIM measure with the DTI and NODDI metrics using randomize, the nonparametric permutation analysis tool in FSL, with TFCE correction for multiple comparisons at $P < 0.05$.

RESULTS

Neuropsychological assessment of patients with mTBI

Table S2 (A and B) displays results for the longitudinal self-report and performance-based cognitive measures at 2 weeks and 6 months after injury for the initial and replication mTBI cohorts. Three of the subjects from the replication cohort were excluded for not having completed the full neuropsychological battery. Overall, patients self-reported a significant reduction in postconcussive symptoms on the RPQ and in disability on the GOSE, but a subset of subjects showed persistent self-reported symptomatology and disability at the 6-month time point. Moreover, patients manifested improved performance in processing speed (TMT) and visuo-perceptive association learning (WAIS coding and symbol) over the 6-month period.

DTI and NODDI voxelwise group comparisons

Cross-sectional analysis between the initial cohort of patients with mTBI versus orthopedic trauma controls and between initial cohort and friend controls at the 2-week time point

Compared to the trauma and healthy controls, the initial mTBI cohort showed lower FA and higher MD in the genu and body of the

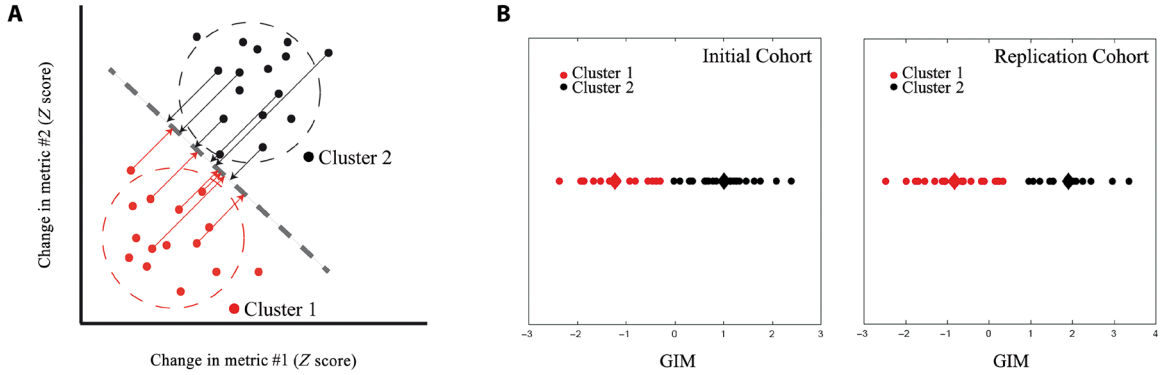

Fig. 2. Machine learning clustering for GIM. (**A**) Two-dimensional schematic illustration of the clustering of change in cognitive and behavioral scores and the principal component analysis projection used to define GIM (arrows for some subjects demonstrating this distance). Participants farther from the line in the upper right direction have better degree of recovery (black points), and participants farther from the line in the other direction have less recovery (red points). (**B**) Representation of the two clusters based on their GIM showing cluster K1 (red; $n = 24$), patients with less recovery, and cluster K2 (black; $n = 16$), patients with more recovery for the initial cohort; and cluster K1 (red; $n = 23$), patients with less recovery, and cluster K2 (black; $n = 14$), patients with more recovery for the replication cohort. The triangles indicate the mean GIM for each cluster.

CC, anterior and posterior limbs of the internal capsule (ALIC and PLIC), anterior corona radiata (ACR), anterior thalamic radiation (ATR), external capsule (EC), and cingulum. FISO was found to be higher in patients versus controls not only for the same tracts but also in the superior longitudinal fasciculi (SLF), posterior corona radiata (PCR), and inferior fronto-occipital fasciculus (IFOF). To a lesser extent in the initial cohort, NDI also showed lower values mainly in the EC, ATR, inferior longitudinal fasciculi (ILF), fornix, and stria terminalis. For NDI, the statistically significant tracts are the same when comparing to the two control groups; however, the extent of significant voxels is greater when comparing to the friend controls (Fig. 3A). Figure 4 shows the mean values, effect sizes (Cohen's *d*), multiple comparisons FDR corrected, and distributions of the sample for FA, MD, NDI, and FISO in the JHU tracts shown to be most affected in the initial mTBI cohort versus ortho controls and versus friend controls for the data-driven voxelwise TBSS analysis.

Longitudinal analysis of patients with mTBI at 2 weeks versus 6 months in the initial and replication mTBI cohorts

Longitudinal voxelwise analysis of patients with mTBI showed decreases over time of NDI in ACR, PCR, posterior thalamic radiation (PTR), ILF, IFOF, ATR, EC, and uncinate fasciculi (Fig 3B). FISO showed decreases over time in the PCR (Fig 3B). NODDI measures were more sensitive to progressive microstructural damage in posterior tracts than DTI, both in the initial and replication cohorts. Mean values and effect sizes, as well as the distribution, for changes of DTI and NODDI over time in the PTR, PCR, and sagittal stratum are displayed in Fig. 5. Results are corrected for multiple comparisons using FDR.

Machine learning analysis

Machine learning clusters among patients with mTBI and their GIM

Two clear clusters were obtained (table S2) dividing the group of patients with mTBI based on their change in self-reported measures (GOSE, RPQ3, and RPQ13) and cognitive-performance measures (WAIS symbol-coding, TMTB-A, and RAVLT). For the initial cohort, cluster K1 included 24 patients who had less improvement on the GIM metric than K2, which consisted of the 16 patients with the best global improvement. For the replication cohort, K1 included 23 patients who had less improvement on the GIM metric than K2, which consisted of the 14 patients with the best global improvement (Fig. 2B). Table S2 (C and D) shows the change from 2 weeks to 6 months after injury in the self-report and cognitive performance measures that comprise the GIM across the 40 initial cohort patients and the 37 replication cohort patients, respectively. While the effect sizes of the change over time appear small, these group averages obscure variation among patients that can be uncovered by the unsupervised machine learning analysis dividing the group into two clusters based on the GIM. It is noteworthy to mention that, because of this division, K1 and K2 differed in years of education only in the initial cohort (K1: $\bar{x} = 14.4$ years, SD ± 2.1; K2: $\bar{x} = 17.7$ years, SD ± 2.5; $P = 0.002$).

Self-report and cognitive measures based on machine learning clustering

Table S2 (C and D) shows the difference between K1 and K2 in each of the measures. The patients from the initial cohort of K2 were much more symptomatic on the RPQ than those of K1 at 2 weeks after injury but recover to symptom levels similar to K1 by 6 months after injury. Similarly, in the replication cohort, K2 patients make a better symptomatic recovery compared to K1 at 6 months. K1 for this replication cohort remains almost at the same level of symptoms over time.

For cognitive performance measures, in the initial cohort, K2 group perform equivalently to K1 at 2 weeks after injury but, at the 6-month time point, are significantly outperforming their K1 counterparts on the RAVLT and the WAIS, particularly the WAIS coding subtest. K2 also trended toward better performance than K1 on the TMTA at both time points. In contrast, for the replication cohort, the patients of K2, despite being more symptomatic on the self-reported measures at 2 weeks, perform better on cognitive testing than K1, except for memory (RAVLT). At 6 months, the K2 group recovered memory to a good average level and overall improve performance in all cognitive areas, whereas the K1 group, despite making slight overall improvement, would drop on executive function (TMTBA) and memory (RAVLT).

Voxelwise group comparison of the DTI and NODDI parameters based on machine learning clustering

No significant relationship between traditional DTI metrics and GIM was found. However, NODDI metrics were associated with

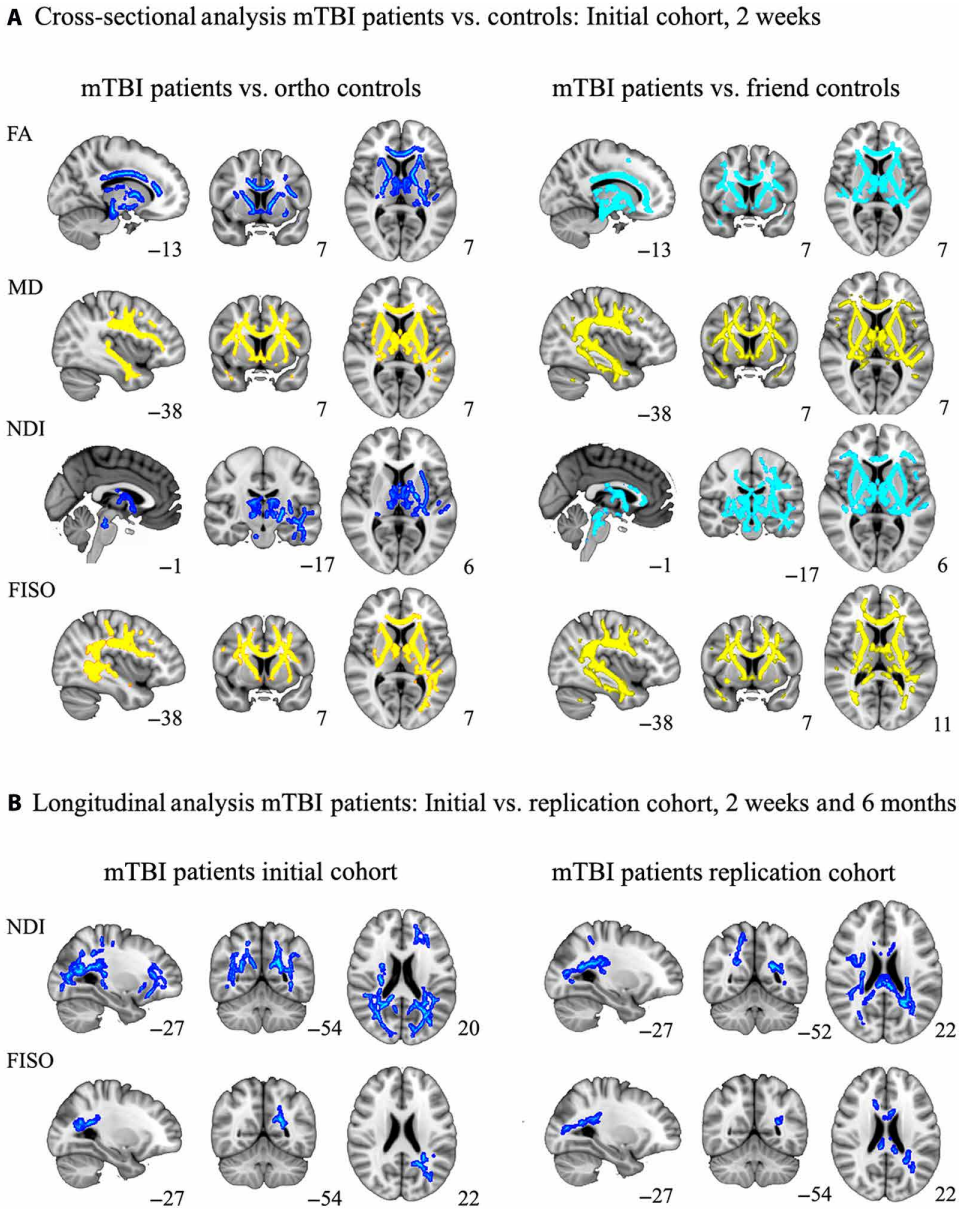

Fig. 3. Cross-sectional and longitudinal voxelwise analysis. An unpaired *t* test was used to compare cross-sectionally the group of patients and orthopedic trauma and friend controls in the voxelwise analysis at 2 weeks. A paired *t* test was used to compare differences among DTI and NODDI measures within the patient mTBI group between 2 weeks and 6 months for each the initial and replication cohorts. (**A**) Left: Cross-sectional voxelwise analysis comparison at 2 weeks between the initial cohort and trauma controls. Right: Cross-sectional voxelwise analysis comparison at 2 weeks between the initial cohort and friend controls. FA, fractional anisotropy; MD, mean diffusivity; ND, neurite dispersion index; FISO, volume fraction of isotropic water. yellow, parameter increased in patients relative to controls; dark/light blue, parameter decreased in patients relative to controls. (**B**) Left: Longitudinal voxelwise comparison between 2 weeks and 6 months after injury in the initial mTBI cohort. Right: Longitudinal voxelwise comparison between 2 weeks and 6 months after injury in the replication mTBI cohort. In dark/light blue, parameter decreased over time. All results corrected for multiple comparisons using TFCE FWE at $P \leq 0.05$. The number next to each image is the MNI atlas coordinate defining its plane.

cluster membership based on GIM in the initial cohort (Fig. 6). The voxelwise group comparison between K1 and K2 revealed increases in FISO in K2 compared to K1, but the pattern of elevated FISO varied between the 2-week and 6-month time points. The increased FISO of K2 versus K1 was posterior predominant at 2 weeks after injury, whereas the increased FISO of K2 versus K1 was anterior predominant at 6 months after injury. In contradistinction, increased ODI of K1 versus K2 was found, both at 2 weeks and at 6 months in a largely stable pattern encompassing much of the central WM tracts, with only the right internal capsule showing resolution of the elevated ODI at 6 months. We did not find significant differences for either DTI or NODDI measures for the replication cohort based on the group division by GIM.

DISCUSSION

The main findings of this study are (i) early lower FA and NDI and early higher MD and FISO in mTBI versus both trauma controls

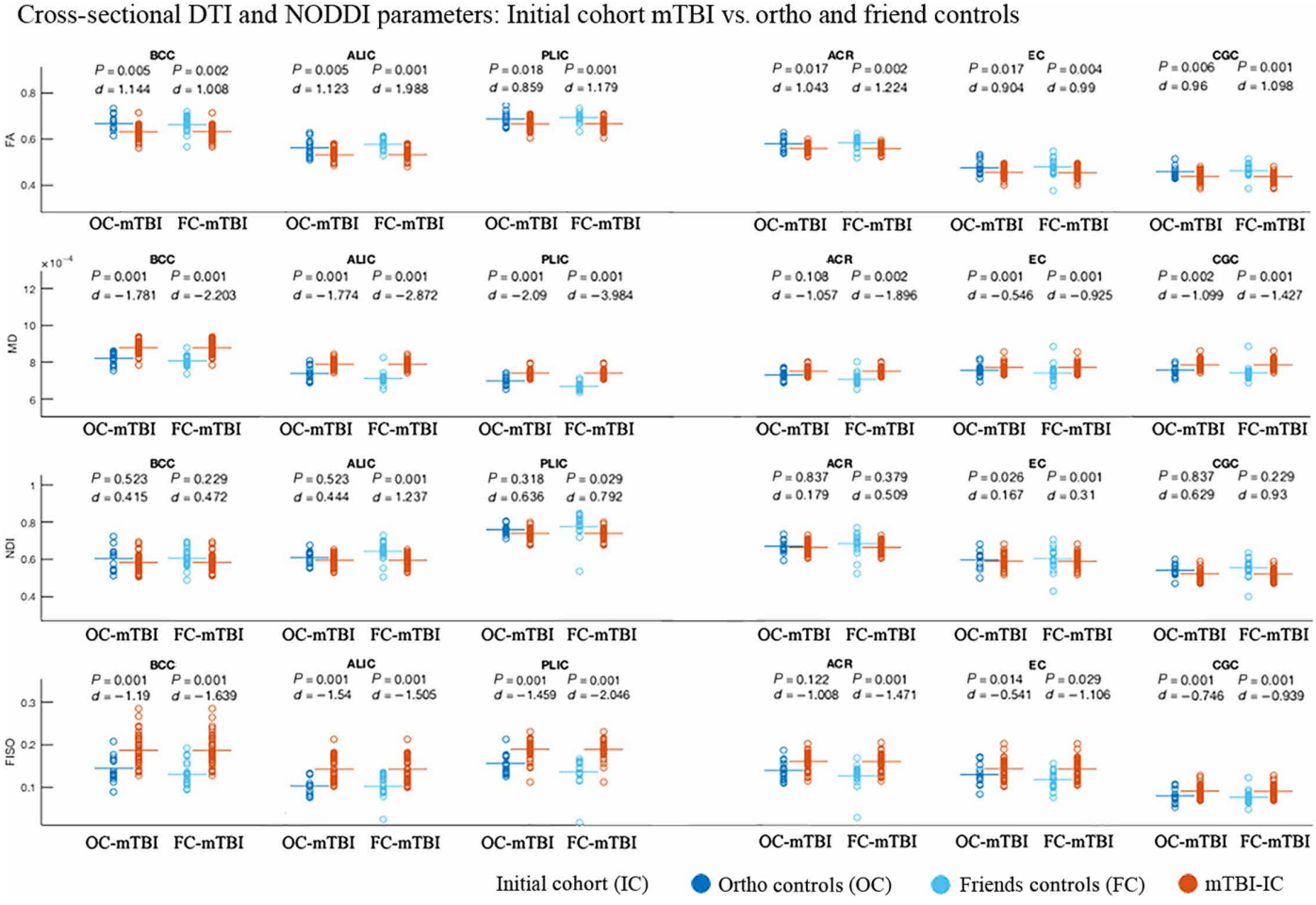

Fig. 4. JHU tracts cross-sectional comparison at 2 weeks between initial mTBI cohort versus ortho controls and friend controls. Averaged FA, MD, NDI, and free water fraction (FISO) values of the left/right JHU tracts for each participant and significant tract at the 2-week time point. BCC, body corpus callosum; ALIC, anterior limb internal capsule; PLIC, posterior limb of internal capsule; ACR, anterior corona radiata; EC, external capsule; CGC, cingulum. Patient and control comparison FDR corrected at $P < 0.05$. *d*, Cohen's *d* effect size.

and friend controls, (ii) longitudinal WM changes of mTBI shown by decreases in NDI and FISO over time, (iii) reduced ODI in those patients with mTBI without symptomatic or cognitive improvement (K1) and dynamically elevated FISO in those patients with mTBI with symptomatic recovery and progressively improved cognitive function (K2), and (iv) robustness of the longitudinal results and the sensitivity of NODDI as a biomarker for progressive WM degeneration due to mTBI, as shown for the results of the replication/generalization cohort.

Traumatic brain injury involves multiple different time-varying pathophysiological effects, including diffuse axonal injury, diffuse microvascular injury, and neuroinflammation, which can lead to neurologic dysfunction (*34*). Because of this complexity, combining different biophysical measurements has potential for characterizing the underlying microarchitectural changes in the brain tissue (*35*). Our cross-sectional DTI findings at the 2-week time point showed lower FA and higher MD in mTBI versus both trauma controls and friend controls, mainly in the frontal and temporal lobes. This agrees with prior DTI studies of early mTBI (*8*, *12*). In addition to these established DTI results, NODDI analysis revealed two additional findings at 2 weeks after injury. First, NDI was lower in patients with mTBI versus both orthopedic trauma controls and friend controls. Second, we found higher FISO values in the same predominantly anterior distribution as FA and MD. The anterior cerebrum undergoes the most angular acceleration from rotational forces since it is farthest from the axis of rotation at the neck; therefore, it may develop the most early edema (high FISO) and axonal injury (low NDI). Overall, these cross-sectional results, which are replicated and generalized across two different control groups without and with non-CNS trauma, suggest that the early lower FA and higher MD values after mTBI is due to an increase in free water content, possibly reflecting neuroinflammation. The sole prior report of DTI and NODDI measurements in TBI, a cross-sectional study of young athletes, found increases in FA and increases in NDI and reduced ODI values (*36*). These results may differ from those found in our study due to the mechanism of injury involving repetitive subconcussive hits over long periods of time, thereby conflating injury and recovery effects, rather than a single episode of mTBI that can be serious enough in some cases to produce anatomic lesions on structural MRI.

Longitudinally, within the group of patients with mTBI, we observed decreases over time in NDI values in both initial and

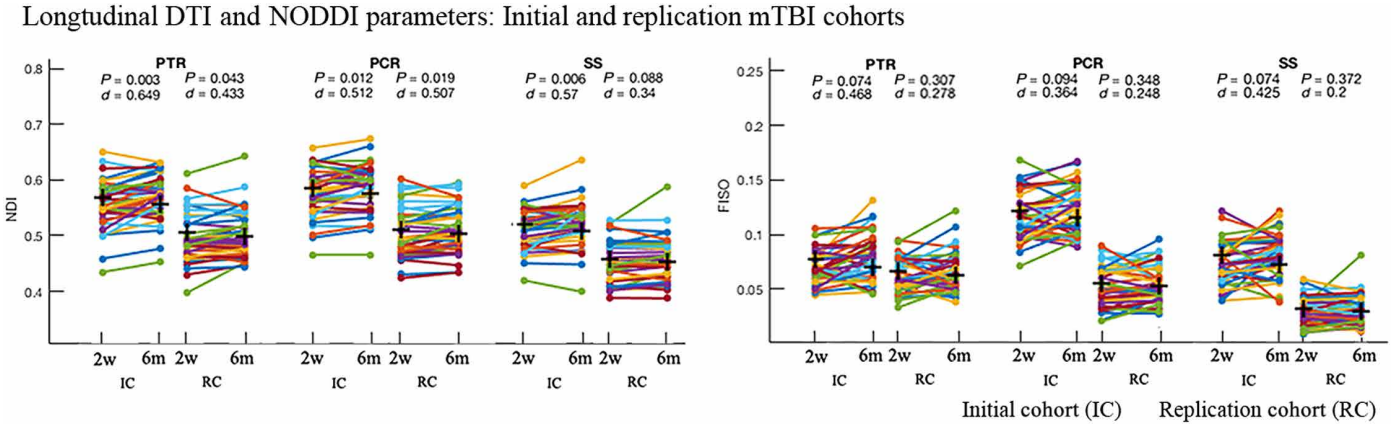

Fig. 5. JHU tracts longitudinal comparison at 2 weeks versus 6 months in mTBI. Averaged NDI and free water fraction (FISO) values of the left/right JHU tracts for each subject at 2-week versus 6-month time points, showing tracts with most significant changes over time mainly in posterior tracts on NDI not captured by the DTI parameters. PTR, posterior thalamic radiation; PCR, posterior corona radiata; SS, sagittal stratum (merged inferior fronto-occipital and ILF). Comparison FDR corrected at $P < 0.05$. *d*, Cohen's *d* effect size.

replication mTBI cohorts, suggesting progressive axonal degeneration, while there were no significant differences in the DTI parameters in either mTBI cohort. Hence, NDI is a more sensitive metric of WM axonal loss than DTI metrics such as FA or MD. The decreases of NDI over time in both mTBI cohorts were primarily in the bilateral posterior periventricular and left anterior periventricular WM. It has been shown that a disproportionately high number of structural connectome links between gray matter areas traverse these regions of deep WM, which form a consistent nexus of network connectivity in the human brain (*37*, *38*). In addition, virtual lesioning of these areas of deep periventricular WM in tractography simulation experiments is particularly disruptive to the overall integrity of the whole-brain WM network, demonstrating their singular importance to the large-scale structural connectome (*39*). Abnormal posterior periventricular WM microstructure is also observed in sensory processing disorders (*40*, *17*) and is the only consistently affected WM region in a meta-analysis of DTI studies of attention-deficit hyperactivity disorder (*41*). Furthermore, the global integrity of the structural connectome is linked to attention and executive function (*42*). This constellation of recent results may account for the major impairments of concussions and mTBI, which are sensitivity to sensory stimuli, attention deficits, and executive dysfunction. Future studies combining microstructural characterization of these posterior periventricular WM tracts with connectomic mapping may prove especially effective for explaining long-term symptomatic, cognitive, and behavioral outcomes after mTBI.

The original result of decreasing WM NDI over time and its replication in a second cohort shows the robustness of NODDI to scanner manufacturer (GE versus Siemens), diffusion pulse sequence (single-band EPI versus multiband EPI), and acquisition protocol (b = 1300 s/mm^2 versus 1000 s/mm^2 for the first shell; 2.7-mm voxel resolution versus 2.4-mm voxel resolution), all of which differed between the two longitudinal mTBI cohorts. Moreover, a prior history of concussions is a common characteristic of patients with mTBI. We think that including patients with previous concussions make the results more generalizable to the entire mTBI population. One advantage of our investigation is the longitudinal approach, which allows us to evaluate for changes over time of the early findings and thereby attribute them to the recent episode of mTBI and not remote earlier ones.

Data-driven machine learning analysis of a composite GIM based on symptom self-report and cognitive performance measures produced two patient clusters in each of the two mTBI cohorts. One cluster was a higher performing subgroup (K2) with early self-reported symptoms that resolved over time who also improved in the information processing speed and verbal memory domains. The other cluster was a lower functioning subgroup (K1) that endorsed relatively few initial symptoms but still performed less well than K2 on the cognitive tests, especially at the 6-month time point. Although no significant DTI differences were seen between these two mTBI subgroups, NODDI showed higher ODI throughout much of the central WM in the K1 group at both time points in the initial mTBI cohort. This greater fiber orientation dispersion in the low functioning K1 cluster may represent a premorbid characteristic influenced by their lower average educational level than K2, implying perhaps lower cognitive reserve. The less well-organized central WM may help explain their poorer cognitive performance compared to the higher functioning K2 cluster. The difference in cognitive and educational levels between the subgroups might also affect symptom reporting. Education is one of the factors that constitute the so-called cognitive reserve, a protective factor associated with better TBI outcome, and it has been reported to be a protective factor at early stages of mTBI, as in the first 24 hours, and regardless of the severity of the TBI (*43*). Specifically, the greater number of symptoms reported by the K2 subgroup at the early time point may partly represent awareness of actual cognitive decline from baseline, followed by eventual return to baseline in both symptoms and cognition by 6 months, at least at the subgroup level if not for every patient. Although the same pattern of symptomatic and cognitive differences was found for the K1 and K2 clusters of the replication cohort, in which K2 reports greater symptoms than K1 initially but the symptom burden of K2 approaches K1 symptoms over time, no significant DTI or NODDI differences were found between the two clusters in this second cohort. This may be because the overall effect size of longitudinal NODDI changes over time was less in the replication cohort than the initial cohort (Fig. 4B) and also because the K2 cluster of the replication cohort did not show as much early cognitive impairment as that of the initial

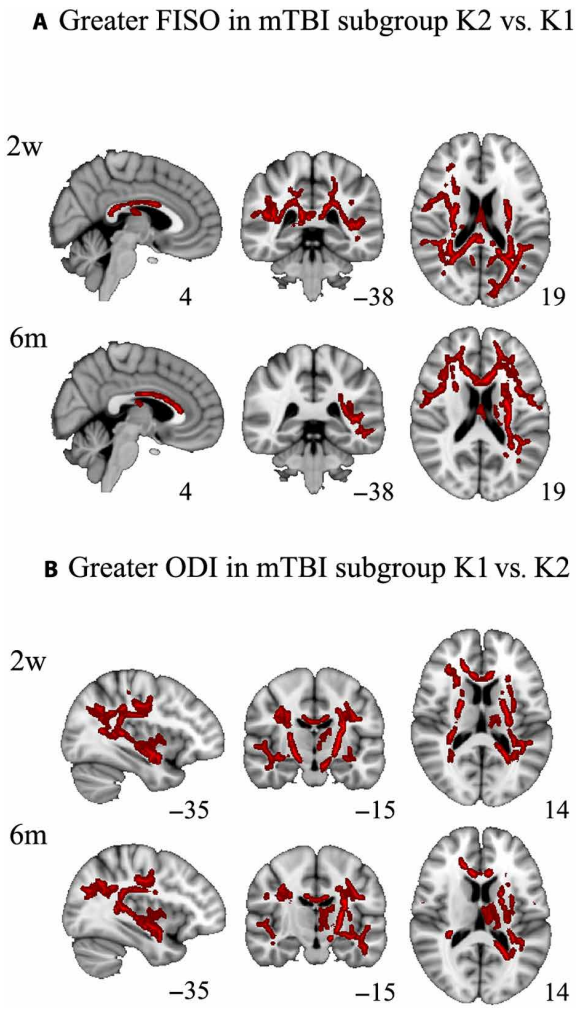

Fig. 6. Voxelwise comparison of NODDI metrics between the initial cohort patients with mTBI subgroups K1 and K2. Voxelwise group comparison of the DTI and NODDI parameters based on the machine learning cluster division (**A**) FISO (volume fraction of isotropic water) increased in patients in cluster 2 (K2). FISO increased in posterior tracts at 2 weeks, while pattern at 6 months showed increases mainly in anterior tracts (**B**) ODI is increased in patients in cluster 1 (K1). All results are corrected for multiple comparisons using TFCE FWE at $P \leq 0.05$. The number next to each image is the MNI atlas coordinate defining its plane.

cohort. Hence, both NODDI and the neurocognitive assessments suggest an overall lesser degree of injury in the replication cohort than the initial cohort. In future studies with larger cohorts, separating function domains (i.e., self-reported measures from cognitive performance) could enable more granular prediction of recovery (*44*).

Another finding was the higher FISO of K2 versus K1 in predominantly posterior WM at 2 weeks after injury versus predominantly anterior WM at 6 months after injury. Because the initial cohort of 40 patients with mTBI showed elevated anterior WM free water, indicating vasogenic edema, at the early time point (Fig. 4A), this means that the K2 subgroup had more extensive early edema than K1 that also included posterior WM. However, the anterior WM edema resolved more slowly in K2 than K1, resulting in the relative elevation of free water in this distribution at the long-term time point. The greater extent of early WM edema corresponds to the greater symptoms reported by the K2 subgroup at that time, with improving edema by 6 months after injury matching their improvement in self-reported and cognitive performance measures. This observed association between WM edema and the trajectory of symptomatic and cognitive recovery after mTBI requires more study to determine whether there is a causal relationship or other cofactors contributing to this symptomatology.

The results replicated in both control groups provide support for our original hypotheses of elevated free water fraction early after injury and of serial decline in WM axonal density during the first 6 months after trauma. The findings show that (i) dynamically increased free water fraction across semiacute and chronic time points was associated with better recovery, suggesting a beneficial role for edema/neuroinflammation; and (ii) statically reduced fiber orientation dispersion was correlated with better long-term cognition, consistent with prior studies showing more highly organized WM in those with better intellectual functioning in multiple domains (*45*–*47*). These new hypotheses from the exploratory findings need to be tested in larger cohorts that have better statistical power for determining imaging-cognition relationships. In the absence of cognitive control data, we also cannot exclude a learning component for the improvement across the two cognitive assessments. Another limitation of the study is the small sample size of the controls, which lack a longitudinal component. The interpretation of change in FISO as vasogenic edema is the best inference we can make at the current time and requires confirmation. In addition, note that TBSS analysis is limited to the core of major WM pathways, and the JHU tract analysis of paired tracts were averages of the right and left sides, perhaps sacrificing information about hemispheric asymmetries to improve statistical power.

In summary, we found that NODDI parameters are sensitive imaging biomarkers for the subtle yet complex underlying WM microstructural pathology after mTBI, such as diffuse axonal injury and neuroinflammation. Our results show that the early lower FA and higher MD values after mTBI, which are primarily in the anterior WM, correspond to WM regions of higher FISO, which may reflect inflammatory vasogenic edema. This elevation of free water is more extensive in the subgroup of patients reporting more postconcussive symptoms early after trauma. The longer-term changes from 2 weeks to 6 months after mTBI are marked by declining neurite density in predominantly posterior WM, suggesting axonal degeneration from DAI for which NODDI appears more sensitive than any of the DTI metrics, such as FA. The affected posterior WM regions are known to be topologically integral to the structural connectome and are involved in multiple sensory and cognitive domains, including attention and executive function. The observation of stably elevated WM fiber orientation in the mTBI subgroup with poorer cognitive performance may represent the sensitivity of ODI to premorbid intellectual functioning. Further research studies in larger well-phenotyped cohorts are needed to validate NODDI biomarkers for mTBI diagnosis, for prediction of self-reported symptoms, cognitive performance, and for treatment monitoring. Moreover, NODDI has been optimized for gray matter (*48*). Studies combining NODDI measurements in WM and gray matter can be of additional value to better characterize patients with mTBI.

SUPPLEMENTARY MATERIALS

Supplementary material for this article is available at http://advances.sciencemag.org/cgi/content/full/6/32/eaaz6892/DC1

View/request a protocol for this paper from *Bio-protocol*.

REFERENCES AND NOTES

1. G. T. Manley, A. I. Maas, Traumatic brain injury: An international knowledge-based approach. *JAMA* **310**, 473–474 (2013).
2. E. D. Bigler, Neuroimaging biomarkers in mild traumatic brain injury (mTBI). *Neuropsychol. Rev.* **23**, 169–209 (2013).
3. H. S. Levin, R. R. Diaz-Arrastia, Diagnosis, prognosis, and clinical management of mild traumatic brain injury. *Lancet Neurol.* **14**, 506–517 (2015).
4. R. Radhakrishnan, A. Garakani, L. S. Gross, M. K. Goin, J. Pine, A. E. Slaby, C. R. Sumner, D. A. Baron, Neuropsychiatric aspects of concussion. *Lancet Psychiatry* **12**, 1166–1175 (2016).
5. P. J. Basser, D. K. Jones, Diffusion-tensor MRI: Theory, experimental design and data analysis – a technical review. *NMR Biomed.* **15**, 456–467 (2002).
6. S. Mori, J. Zhang, Principles of diffusion tensor imaging and its applications to basic neuroscience research. *Neuron* **51**, 527–539 (2006).
7. P. Mukherjee, J. I. Berman, S. W. Chung, C. P. Hess, R. G. Henry, Diffusion tensor MR imaging and fiber tractography: Theoretic underpinnings. *AJNR Am. J. Neuroradiol.* **29**, 632–641 (2008).
8. E. L. Yuh, S. R. Cooper, P. Mukherjee, J. K. Yue, H. F. Lingsma, W. A. Gordon, A. B. Valadka, D. O. Okonkwo, D. M. Schnyer, M. J. Vassar, A. I. Maas, G. T. Manley; TRACK-TBI INVESTIGATORS, Diffusion tensor imaging for outcome prediction in mild traumatic brain injury: A TRACK-TBI study. *J. Neurotrauma* **31**, 1457–1477 (2014).
9. I. D. Croall, C. J. Cowie, J. He, A. Peel, J. Wood, B. S. Aribisala, P. Mitchell, A. D. Mendelow, F. E. Smith, D. Millar, T. Kelly, A. M. Blamire, White matter correlates of cognitive dysfunction after mild traumatic brain injury. *Neurology* **83**, 494–501 (2014).
10. L. Oehr, J. Anderson, Diffusion-tensor imaging findings and cognitive function following hospitalized mixed-mechanism mild traumatic brain injury: A systematic review and meta-analysis. *Arch. Phys. Med. Rehabil.* **11**, 2308–2319 (2017).
11. D. K. Jones, M. Cercignani, Twenty-five pitfalls in the analysis of diffusion MRI data. *NMR Biomed.* **23**, 803–820 (2010).
12. C. Eierud, R. C. Craddock, S. Fletcher, M. Aulakh, B. King-Casas, D. Kuehl, S. M. LaConte, Neuroimaging after mild traumatic brain injury: Review and meta-analysis. *Neuroimage Clin.* **4**, 283–294 (2014).
13. H. Zhang, P. L. Hubbard, G. J. Parker, D. C. Alexander, Axon diameter mapping in the presence of orientation dispersion with diffusion MRI. *Neuroimage* **56**, 1301–1315 (2011).
14. O. I. Jelescu, M. D. Budde, Design and validation of diffusion MRI models of white matter. *Front. Phys.* **61**, 61 (2017).
15. F. Sepehrband, K. A. Clark, J. F. Ullmann, N. D. Kurniawan, G. Leanage, D. C. Reutens, Z. Yang, Brain tissue compartment density estimated using diffusion-weighted MRI yields tissue parameters consistent with histology. *Hum. Brain Mapp.* **36**, 3687–3702 (2015).
16. K. Sato, A. Kerever, K. Kamagata, K. Tsuruta, R. Irie, K. Tagawa, H. Okazawa, E. Arikawa-Hirasawa, N. Nitta, I. Aoki, S. Aoki, Understanding microstructure of the brain by comparison of neurite orientation dispersion and density imaging (NODDI) with transparent mouse brain. *Acta Radiol. Open* **6**, 2058460117703816 (2017).
17. Y. S. Chang, J. P. Owen, N. J. Pojman, T. Thieu, P. Bukshpun, M. L. Wakahiro, J. I. Berman, T. P. Roberts, S. S. Nagarajan, E. H. Sherr, P. Mukherjee, White matter changes of neurite density and fiber orientation dispersion during human brain maturation. *PLOS ONE* **10**, e0123656 (2015).
18. A. Mah, B. Geeraert, C. Lebel, Detailing neuroanatomical development in late childhood and early adolescence using NODDI. *PLOS ONE* **12**, e0182340 (2017).
19. T. Billiet, M. Vandenbulcke, B. Mädler, R. Peeters, T. Dhollander, H. Zhang, S. Deprez, B. R. Van den Bergh, S. Sunaert, L. Emsell, Age-related microstructural differences quantified using myelin water imaging and advanced diffusion MRI. *Neurobio. Aging* **36**, 2107–2121 (2015).
20. I. Timmers, A. Roebroeck, M. Bastiani, B. Jansma, E. Rubio-Gozalbo, H. Zhang, Assessing microstructural substrates of white matter abnormalities: A comparative study using DTI and NODDI. *PLOS ONE* **11**, e0167884 (2016).
21. K. Kamagata, A. Zalesky, T. Hatano, R. Ueda, M. A. Di Biase, A. Okuzumi, K. Shimoji, M. Hori, K. Caeyenberghs, C. Pantelis, N. Hattori, S. Aoki, Gray matter abnormalities in idiopathic Parkinson's disease: Evaluation by diffusional kurtosis imaging and neurite orientation dispersion and density imaging. *Hum. Brain Mapp.* **38**, 3704–3722 (2017).
22. E. Caverzasi, N. Papinutto, A. Castellano, A. H. Zhu, P. Scifo, M. Riva, L. Bello, A. Falini, A. Bharatha, R. G. Henry, Neurite orientation dispersion and density imaging color maps to characterize brain diffusion in neurologic disorders. *J. Neuroimaging* **26**, 494–498 (2016).
23. T. Schneider, W. Brownlee, H. Zhang, O. Ciccarelli, D. H. Miller, C. G. Wheeler-Kingshott, Sensitivity of multi-shell NODDI to multiple sclerosis white matter changes: A pilot study. *Funct. Neurol.* **32**, 97–101 (2017).
24. G. Lerma-Usabiaga, P. Mukherjee, Z. Ren, M. L. Perry, B. A. Wandell, Replication and generalization in applied neuroimaging. *Neuroimage* **26**, 116048 (2019).
25. J. K. Yue, M. J. Vassar, H. F. Lingsma, S. R. Cooper, D. O. Okonkwo, A. B. Valadka, W. A. Gordon, A. I. Maas, P. Mukherjee, E. L. Yuh, A. M. Puccio, D. M. Schnyer, G. T. Manley; TRACK-TBI Investigators, Transforming research and clinical knowledge in traumatic brain injury pilot: Multicenter implementation of the common data elements for traumatic brain injury. *J. Neurotrauma* **30**, 1831–1844 (2013).
26. American Congress of Rehabilitation Medicine (ACRM), Mild Traumatic Brain Injury Committee, Definition of mild traumatic brain injury. *J. Head Trauma Rehabil.* **8**, 86–87 (1993).
27. M. D. Lezak, D. B. Howieson, E. D. Bigler, D. Tranel, *Neuropsychological Assessment* (Oxford Univ. Press, ed. 5, 2012).
28. E. L. Yuh, P. Mukherjee, H. F. Lingsma, J. K. Yue, A. R. Ferguson, W. A. Gordon, A. B. Valadka, D. M. Schnyer, D. O. Okonkwo, A. I. Maas, G. T. Manley; TRACK-TBI Investigators, Magnetic resonance imaging improves 3-month outcome prediction in mild traumatic brain injury. *Ann. Neurol.* **73**, 224–235 (2013).
29. S. M. Smith, Fast robust automated brain extraction. *Hum. Brain Mapp.* **17**, 143–155 (2002).
30. J. P. Owen, Y. S. Chang, N. J. Pojman, P. Bukshpun, M. L. Wakahiro, E. J. Marco, J. I. Berman, J. E. Spiro, W. K. Chung, R. L. Buckner, T. P. Roberts, S. S. Nagarajan, E. H. Sherr, P. Mukherjee; Simons VIP Consortium, Aberrant white matter microstructure in children with 16p11.2 deletions. *J. Neurosci.* **34**, 6214–6223 (2014).
31. M. Jenkinson, P. Bannister, M. Brady, S. Smith, Improved optimization for the robust and accurate linear registration and motion correction of brain images. *Neuroimage* **17**, 825–841 (2002).
32. T. E. Nichols, A. P. Holmes, Nonparametric permutation tests for functional neuroimaging: A primer with examples. *Hum. Brain Mapp.* **15**, 1–25 (2002).
33. P. J. McMahon, A. Hricik, J. K. Yue, A. M. Puccio, T. Inoue, H. F. Lingsma, S. R. Beers, W. A. Gordon, A. B. Valadka, G. T. Manley, D. O. Okonkwo; TRACK-TBI Investigators, Symptomatology and functional outcome in mild traumatic brain injury: Results from the prospective TRACK-TBI study. *J. Neurotrauma* **31**, 26–33 (2014).
34. E. D. Bigler, Neuropathology of mild traumatic brain injury: correlation to neurocognitive and neurobehavioral findings, in *Brain Neurotrauma: Molecular, Neuropsychological, and Rehabilitation Aspects*, F. H. Kobeissy, ed. (Boca Raton, FL, CRC Press/Taylor & Francis, 2015), Chap. 31.
35. M. Cercignani, S. Bouyagoub, Brain microstructure by multi-modal MRI: Is the whole greater than the sum of its parts? *Neuroimage* **15**, 117–127 (2018).
36. N. W. Churchill, E. Caverzasi, S. J. Graham, M. G. Hutchison, T. A. Schweizer, White matter microstructure in athletes with a history of concussion: Comparing diffusion tensor imaging (DTI) and neurite orientation dispersion and density imaging (NODDI). *Hum. Brain Mapp.* **38**, 4201–4211 (2017).
37. J. P. Owen, Y. S. Chang, P. Mukherjee, Edge density imaging: Mapping the anatomic embedding of the structural connectome within the white matter of the human brain. *Neuroimage* **109**, 402–417 (2015).
38. J. P. Owen, M. B. Wang, P. Mukherjee, Periventricular white matter is a nexus for network connectivity in the human brain. *Brain Connect.* **6**, 548–557 (2016).
39. M. B. Wang, J. P. Owen, P. Mukherjee, A. Raj, Brain network eigenmodes provide a robust and compact representation of the structural connectome in health and disease. *PLOS Comput. Biol.* **13**, e1005550 (2017).
40. J. P. Owen, E. J. Marco, S. Desai, E. Fourie, J. Harris, S. S. Hill, A. B. Arnett, P. Mukherjee, Abnormal white matter microstructure in children with sensory processing disorders. *Neuroimage Clin.* **2**, 844–853 (2013).
41. L. Chen, X. Hu, L. Ouyang, N. He, Y. Liao, Q. Liu, M. Zhou, M. Wu, X. Huang, Q. Gong, A systematic review and meta-analysis of tract-based spatial statistics studies regarding attention-deficit/hyperactivity disorder. *Neurosci. Biobehav. Rev.* **68**, 838–847 (2016).
42. M. Xiao, H. Ge, B. S. Khundrakpam, J. Xu, G. Bezgin, Y. Leng, L. Zhao, Y. Tang, X. Ge, S. Jeon, W. Xu, A. C. Evans, S. Liu, Attention performance measured by attention network test is correlated with global and regional efficiency of structural brain networks. *Front. Behav. Neurosci.* **10**, 194 (2016).
43. M. G. de Freitas Cardoso, R. M. Faleiro, J. J. de Paula, A. Kummer, P. Caramelli, A. L. Teixeira, L. C. de Souza, A. S. Miranda, Cognitive impairment following acute mild traumatic brain injury. *Front. Neurol.* **8**, 198 (2019).
44. H. S. Levin, X. Li, S. R. McCauley, G. Hanten, E. A. Wilde, P. Swank, Neuropsychological outcome of mTBI; A principal component analysis approach. *J. Neurotrauma* **30**, 625–632 (2013).
45. A. M. Fjell, L. T. Westlye, I. K. Amlien, K. B. Walhovd, Reduced white matter integrity is related to cognitive instability. *J. Neurosci.* **31**, 18060–18072 (2011).
46. Y. Yang, A. R. Bender, N. Raz, Age related differences in reaction time components and diffusion properties of normal-appearing white matter in healthy adults. *Neuropsychologia* **66**, 246–258 (2015).
47. R. A. Kievit, S. W. Davis, J. Griffiths, M. M. Correia, Cam-Can, R. N. Henson, A watershed model of individual differences in fluid intelligence. *Neuropsychologia* **91**, 186–198 (2016).

48. H. Fukutomi, M. F. Glasser, K. Murata, T. Akasaka, K. Fujimoto, T. Yamamoto, J. A. Autio, T. Okada, K. Togashi, H. Zhang, D. C. Van Essen, T. Hayashi, Diffusion tensor model links to neurite orientation dispersion and density imaging at high b-value in cerebral cortical gray matter. *Sci. Rep.* **9**, 12246 (2019).

Acknowledgments

Funding: The TRACK-TBI study was funded by the U.S. NIH, National Institute of Neurological Disorders and Stroke (NINDS) (grant no.U01 NS086090), the U.S. Department of Defense (DoD) TBI Endpoints Development (TED) Initiative (grant no.W81XWH-14-2-0176), OneMind, and NeuroTrauma Sciences LLC. **Author contributions:** Conception and design of the study: E.M.P, J.P.O., E.L.Y., M.B.W., and P.M. Acquisition and analysis of the data: E.M.P., J.P.O., and M.B.W. Drafting significant portion of the manuscript and figures: E.M.P., J.P.O., M.J.V., A.R.F, R.D.-A, J.T.G., D.O.O., C.S.R., M.B.S, N.T., S.J., M.M., C.L.M.D., H.S.L., G.T.M., and P.M. **Competing interests:** P.M. reported grants from GE Healthcare and nonfinancial support from GE-NFL Head Health Initiative outside the submitted work. In addition, P.M. had a patent for USPTO no. 62/269,778 pending outside the submitted work. C.S.R. reported grants from the NIH and DoD during the conduct of the study. L.N. reported grants from DoD during the conduct of the study, grants from NIH, grants from Medical College of Wisconsin Center for Patient Care and Outcomes Research, grants from Advancing a Healthier Wisconsin, and grants from the DoD outside the submitted work. N.T. reported grants from NIH-NINDS during the conduct of the study. J.T.G reported grants from the NIH-NINDS during the conduct of the study. E.L.Y. reported grants from the University of California, San Francisco during the conduct of the study; in addition, E.L.Y. had a patent for USPTO no. 62/269,778 pending outside the submitted work. A.R.F. reported grants from the NIH/NINDS, the DoD, Veterans Affairs, Craig H. Neilsen Foundation, Wings for Life Foundation, and the Department of Energy during the conduct of the study. M.M. reported grants from the NIH and DoD during the conduct of the study. M.B.S. reported personal fees from Aptinyx, Bionomics, Janssen, and Neurocrine, as well as personal fees and stock options from Oxeia Biopharmaceuticals outside the submitted work. R.D.A. reported personal fees and research funding from Neural Analytics Inc. and travel reimbursement from Brain Box Solutions Inc. outside the submitted work. C.L.M.D. reported grants from NIH-NINDS, National Institute of Aging, and the DoD during the conduct of the study. G.T.M. reported grants from the NINDS during the conduct of the study, research funding from the U.S. Department of Energy, grants from the DoD, research funding from Abbott Laboratories, grants from the National Football League Scientific Advisory Board, and research funding from One Mind. In addition, G.T.M. had a patent for had a patent for USPTO no. 62/269,778 pending outside the submitted work. He served for two seasons as an unaffiliated neurologic consultant for home games of the Oakland Raiders and was compensated $1500 per game for six games during the 2017 season but received no compensation for this work during the 2018 season. O. Adeoye reported grants from the NIH-NINDS during the conduct of the study. K. Boase reported grants from TRACK-TBI Grant during the conduct of the study. Y. Bodien reported grants from Spaulding Rehabilitation Hospital during the conduct of the study. J. D. Corrigan reported grants from University of California, San Francisco during the conduct of the study. A.-C. Duhaime reported grants from the NIH during the conduct of the study. V. R. Feeser reported grants from Virginia Commonwealth University during the conduct of the study. R. Merchant and A. Valadka are TRACK-TBI investigators at Virginia Commonwealth University. D. Goldman reported grants from the NINDS and USC Schaeffer Center during the conduct of the study and personal fees from Amgen, Avanir Pharmaceuticals, Acadia Pharmaceuticals, Aspen Health Strategy Group, and Celgene outside the submitted work. S. Gopinath reported grants from the NIH and DoD during the conduct of the study. N. Kreitzer reported personal fees from Portola outside the submitted work. C. Lindsell reported grants from the NIH during the conduct of the study. J. Machamer reported grants from the NIH during the conduct of the study. C. Madden reported grants from the NIH TRACK-TBI Study and One Mind for Research during the conduct of the study. T. McAllister reported grants from UCSF from the NIH and the National Collegiate Athletic Association and the DoD during the conduct of the study. J. Rosand reported grants from the NIH during the conduct of the study and personal fees from Boehringer Ingelheim and New Beta Innovations outside the submitted work. A. Sander reported grants from the NIH during the conduct of the study. M. Sherer reported receiving partial funding through a grant for this study. P. Vespa reported grants from the NIH during the conduct of the study. R. Zafonte received royalties from Oakstone for an educational CD (Physical Medicine and Rehabilitation: A Comprehensive Review) and Demos publishing for serving as coeditor of Brain Injury Medicine. R. Zafonte serves or served on the scientific advisory boards of Myomo, Oxeia Biopharma, Biodirection, and Elminda and also evaluates patients in the MGH Brain and Body-TRUST Program, which is funded by the National Football League Players Association. R. Zafonte had served on the Mackey White Committee. **Data and materials availability:** All data needed to evaluate the conclusions in the paper are present in the paper and/or the Supplementary Materials. Additional data related to this paper may be requested from the authors.

Submitted 1 October 2019
Accepted 26 June 2020
Published 7 August 2020
10.1126/sciadv.aaz6892

Citation: E. M. Palacios, J. P. Owen, E. L. Yuh, M. B. Wang, M. J. Vassar, A. R. Ferguson, R. Diaz-Arrastia, J. T. Giacino, D. O. Okonkwo, C. S. Robertson, M. B. Stein, N. Temkin, S. Jain, M. McCrea, C. L. MacDonald, H. S. Levin, G. T. Manley, P. Mukherjee, TRACK-TBI Investigators, The evolution of white matter microstructural changes after mild traumatic brain injury: A longitudinal DTI and NODDI study. *Sci. Adv.* **6**, eaaz6892 (2020).